

## Contribution of the Selectivity Filter to Inactivation in Potassium Channels

Laszlo Kiss, Joseph LoTurco, and Stephen J. Korn

Department of Physiology and Neurobiology, University of Connecticut, Storrs, Connecticut 06269 USA

**ABSTRACT** Voltage-gated  $K^+$  channels exhibit a slow inactivation process, which becomes an important influence on the rate of action potential repolarization during prolonged or repetitive depolarization. During slow inactivation, the outer mouth of the permeation pathway undergoes a conformational change. We report here that during the slow inactivation process, the channel progresses through at least three permeation states; from the initial open state that is highly selective for  $K^+$ , the channel enters a state that is less permeable to  $K^+$  and more permeable to  $Na^+$ , and then proceeds to a state that is non-conducting. Similar results were obtained in three different voltage-gated  $K^+$  channels: Kv2.1, a channel derived from *Shaker* (*Shaker*  $\Delta$  A463C), and a chimeric channel derived from Kv2.1 and Kv1.3 that displays classical C-type inactivation. The change in selectivity displayed both voltage- and time-dependent properties of slow inactivation and was observed with  $K^+$  on either side of the channel. Elevation of internal  $[K^+]$  inhibited  $Na^+$  conduction through the inactivating channel in a concentration-dependent manner. These results indicate that the change in selectivity filter function is an integral part of the slow inactivation mechanism, and argue against the hypothesis that the inactivation gate is independent from the selectivity filter. Thus, these data suggest that the selectivity filter is itself the inactivation gate.

### INTRODUCTION

In response to prolonged or repetitive depolarization, voltage-gated  $K^+$  channels enter an inactivated state in which  $K^+$  conductance is prevented. Inactivation involves at least two different mechanisms, an N-type mechanism that occurs at the cytoplasmic face of the channel (Hoshi et al., 1990; Zagotta et al., 1990) and a C-type mechanism that involves a conformational change near the outer mouth of the pore (Grissmer and Cahalan, 1989; Yellen et al., 1994; Liu et al., 1996). Although the C-type mechanism occurs with a wide range of rates, it is generally much slower than the N-type mechanism and occurs on a time scale of 10s of ms to seconds (Stuhmer et al., 1989; Hoshi et al., 1991; Lopez-Barneo et al., 1993; Marom and Levitan, 1994). In neurons, entry of  $K^+$  channels into the C-type inactivated state can lead to significant changes in signaling properties such as firing rate and action potential duration (Aldrich et al., 1979; Aldrich, 1981; Hsu et al., 1993). Consequently, mechanisms that control the rate and underlie phenotypic diversity of C-type inactivation are of considerable importance to the physiology of cells that utilize long duration action potentials or undergo changes in firing frequency.

Several lines of evidence suggest that C-type inactivation involves a constriction within the outer mouth of the pore. C-type inactivation results from a cooperative conformational change involving all four subunits of the channel (Ogielska et al., 1995; Panyi et al., 1995). During inactivation, cysteines at *Shaker* position 448 (located just external

to the selectivity filter GYG residues) can become cross-linked, which suggests that the molecular movement associated with inactivation brings these amino acid residues closer together (Liu et al., 1996). Occupancy of the outer mouth of the pore by tetraethylammonium, which binds near the amino acid at *Shaker* position 449 (MacKinnon and Yellen, 1990; Heginbotham and MacKinnon, 1992), or protonation of a histidine at the equivalent of *Shaker* position 449, slow the rate of C-type inactivation (Busch et al., 1991; Choi et al., 1991). Similarly, occupancy of the outer mouth of the pore by  $K^+$  slows the rate of C-type inactivation (Lopez-Barneo et al., 1993; Baukowitz and Yellen, 1996). It has been proposed that this slowing occurs by a “foot-in-the-door” mechanism, whereby the presence of the cationic  $K^+$ , tetraethylammonium, or  $H^+$  within the pore, just external to the selectivity filter, prevents the constriction required for inactivation to occur. At submillimolar internal  $[K^+]$ , the relative permeability of *Shaker* to  $K^+$  and  $Na^+$  changes during the C-type inactivation process (Starkus et al., 1997), which suggests that the inactivation-induced conformational change can influence ionic selectivity.

The site at which  $K^+$  directly slows inactivation appears to be a high affinity binding site involved in the ionic selectivity mechanism (Kiss and Korn, 1998). Recent structural data from the *Streptomyces lividans*  $K^+$  channel suggest that the high affinity  $K^+$  binding site associated with selectivity is in the narrow region of the conduction pathway that forms the selectivity filter (Doyle et al., 1998). Taken together, these observations lead to the hypothesis that slow inactivation results from a constriction of the selectivity filter itself.

To test this hypothesis, we examined the inactivation-induced change in ionic selectivity in three channels. We studied Kv2.1, which is the one wild-type  $K^+$  channel known to display a competitive interaction between  $K^+$  and

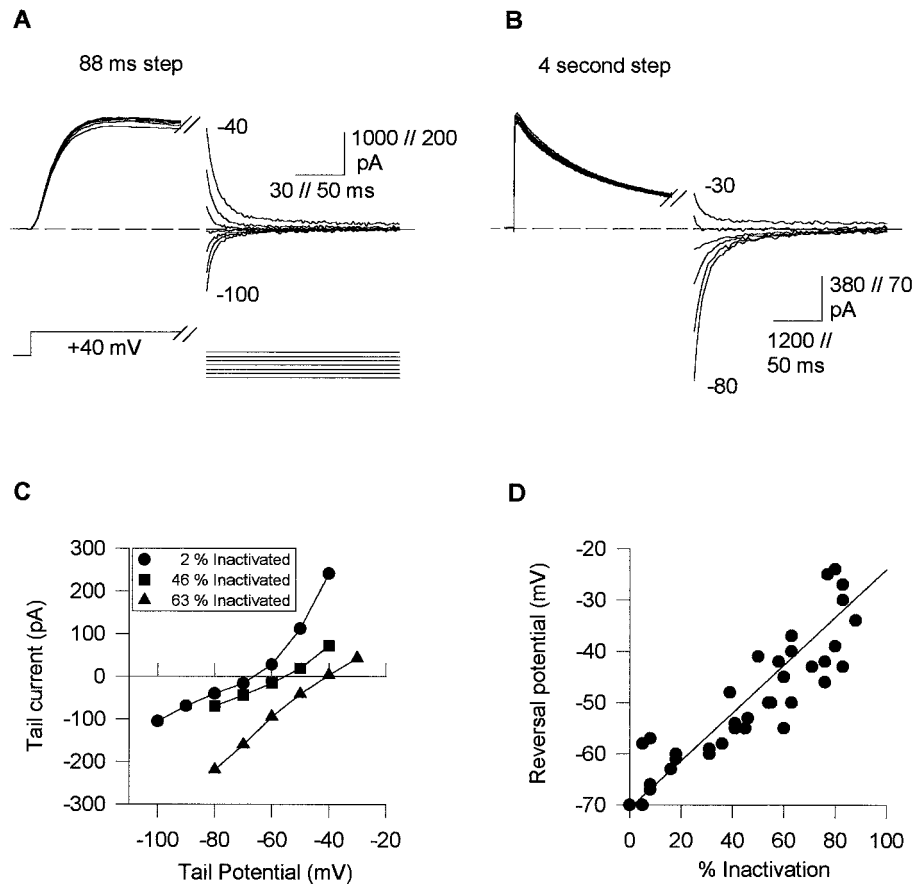
Received for publication 9 June 1998 and in final form 1 October 1998.

Address reprint requests to Dr. Stephen Korn, Department of Physiology and Neurobiology, Box U-156, University of Connecticut 3107 Horsebarn Hill Road, Storrs, CT 06269. Tel.: 860-486-4554; Fax: 860-486-3303; E-mail: korn@oracle.pnb.uconn.edu.

© 1999 by the Biophysical Society

0006-3495/99/01/253/11 \$2.00

**FIGURE 1** Change in current reversal potential in Kv2.1 during inactivation. (A) Cells were depolarized to +40 mV for 88 ms, followed by repolarization in 10-mV increments to different potentials between -100 and -40 mV. The time and current calibrations are different for step and tail currents. (B) Same experiment (and cell) as in A except that the activating depolarization lasted for 4 s. Tail currents shown were evoked by repolarization to potentials between -80 and -30 mV. (C) "Instantaneous" current-voltage (I-V) relationships from the cell described in panels A and B, following depolarizations that produced 2, 46, and 63% inactivation. (D) Reversal potential as a function of % inactivation. Data represent 13 cells from which reversal potentials were measured following depolarization for either two or three different durations.



$\text{Na}^+$  for occupancy of the selectivity filter (Korn and Ikeda, 1995) but which displays a nonclassical slow inactivation process (De Biasi et al., 1993). We also studied a chimeric channel derived from Kv2.1 and Kv1.3, which displays both competition between  $\text{K}^+$  and  $\text{Na}^+$  for the selectivity filter and also a classical C-type inactivation mechanism (Kiss and Korn, 1998). Finally, we examined a *Shaker* mutant, *Shaker*  $\Delta$  A463C, which conducts  $\text{Na}^+$  better than wild-type *Shaker*, displays competition between  $\text{K}^+$  and  $\text{Na}^+$  for the selectivity filter, and displays slow inactivation similar to wild-type *Shaker* (Ogielska and Aldrich, 1996). In each channel, prolonged depolarization produced a change in ionic selectivity that displayed the voltage- and time-dependent properties of slow inactivation. During inactivation,  $\text{Na}^+$  permeability first increased relative to  $\text{K}^+$  permeability, and then  $\text{Na}^+$  permeability was reduced. This selectivity change occurred with  $\text{K}^+$  on either side of the membrane. Together, these data indicate that the selectivity filter is an integral part of the inactivation mechanism and argue against the hypothesis that the inactivation gate is external to and independent from the selectivity filter. Thus, these data support the hypothesis that the selectivity filter itself is the inactivation gate.

## MATERIALS AND METHODS

### Molecular biology and channel expression

All methodology has been previously published (Kiss et al., 1998; Kiss and Korn, 1998). We studied three cloned  $\text{K}^+$  channels, the wild-type Kv2.1,

a chimeric channel that contained the S5-S6 loop from Kv1.3 inserted into a backbone of Kv2.1 (Gross et al., 1994; Kiss et al., 1998), and *Shaker*  $\Delta$  A463C, (*Shaker* H4 with mutations  $\Delta$ 6-46 to remove N-type inactivation and A463C to enhance  $\text{Na}^+$  permeability; Hoshi et al., 1990; Ogielska and Aldrich, 1996). Briefly,  $\text{K}^+$  channel cDNA was subcloned into pcDNA3 vector and expressed in the human embryonic kidney cell line, HEK293 cells (American Type Culture Collection, Rockville, MD) by electroporation. Cells were maintained in Dulbecco's modified Eagle's medium plus 10% fetal bovine serum plus 1% penicillin/streptomycin (maintenance media); new cells were brought up from frozen stock every 6 weeks. Cells were co-transfected by electroporation with channel plasmid (15  $\mu\text{g}/0.2$  ml) and the CD8 antigen (1  $\mu\text{g}/0.2$  ml). After electroporation, cells were plated on protamine-coated glass coverslips submerged in maintenance media. Electrophysiological recordings were made 18-30 h after transfection. On the day of recording, cells were washed with fresh media and incubated with Dynabeads M450 conjugated with antibody to CD8 (1  $\mu\text{l}/\text{ml}$ ; Dynal, Oslo, Norway) for visualization of transfected cells (Jurman et al., 1994). Electroporated but untransfected HEK cells had less than 2 nS endogenous  $\text{K}^+$  conductance with 140 mM internal  $\text{K}^+$ , which is 1000-5000 fold lower than in cells transfected with  $\text{K}^+$  channels. Untransfected HEK cells had no resolvable  $\text{Na}^+$  currents with 165 mM external  $\text{Na}^+$ , with or without internal  $\text{K}^+$ .

### Electrophysiology

Electrophysiological methods were as described previously (Kiss and Korn, 1998). All recordings were made in the whole cell or in the excised outside-out patch configuration. In all experiments, the holding potential was -80 mV. Depolarizing stimuli are illustrated in the figures. Currents were filtered at 2 kHz (internal Axopatch filter; Axon Instruments, Foster City, CA). Internal solutions in all experiments contained: 140 mM XCl ( $X = \text{K}^+$ ,  $\text{Na}^+$ , Tris, or *N*-methyl glucamine (NMG $^+$ )), 20 mM HEPES, 10

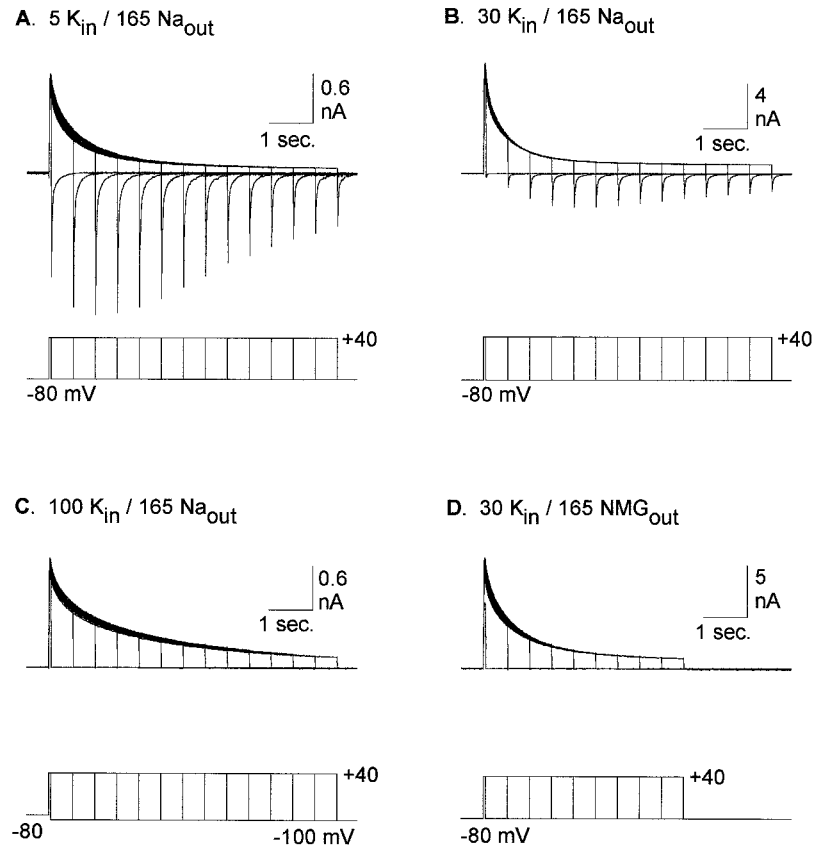


**FIGURE 2** Enhanced inward current during inactivation is not caused by external accumulation of  $K^+$ . Depolarizing voltage steps to +40 mV were delivered for incrementally increasing durations, once every 35 s. The first depolarization lasted for 50 ms, and the duration of depolarization for each sequential trace increased in 500 ms increments. (A–C) Fourteen superimposed traces that illustrate currents evoked in the presence of 5 (A), 30 (B), and 100 mM (C) internal  $K^+$ . A and B illustrate whole cell currents; currents in C were evoked in an excised, outside-out patch. Repolarization was to  $-80$  mV in A and B, and to  $-100$  mV in C. (D) Currents evoked in the presence of 30 mM internal  $K^+$  and 0 external  $Na^+$  (NMG $^+$  substitution).

mM EGTA, 1 mM  $CaCl_2$ , 4 mM  $MgCl_2$ , pH 7.3, osmolality 285. External solutions contained: 165 mM XCl, 20 mM HEPES, 10 mM glucose, 2 mM  $CaCl_2$ , 1 mM  $MgCl_2$ , pH 7.3, osmolality 320. Substitutions are listed in the figure legends. Solutions containing low  $[K^+]$  or  $[Na^+]$  were osmotically balanced with Tris or NMG $^+$ . Solutions were fed from one of six reservoirs through plastic tubing to a single, 100  $\mu$ m diameter quartz tip placed within 10  $\mu$ m of the cell. The solution bathing the cell was constantly flowing, and switched manually.

Summed data are expressed as mean  $\pm$  SE. Percent inactivation of  $K^+$  currents was calculated as the magnitude of the current at the end of the depolarizing voltage step divided by the magnitude of the current at the peak. All data acquisition, analysis, and curve fitting were done with Clampfit (Axon Instruments) and Sigmaplot 2.0 (Jandel Scientific).

## RESULTS

### Change in ionic selectivity of Kv2.1 with prolonged depolarization

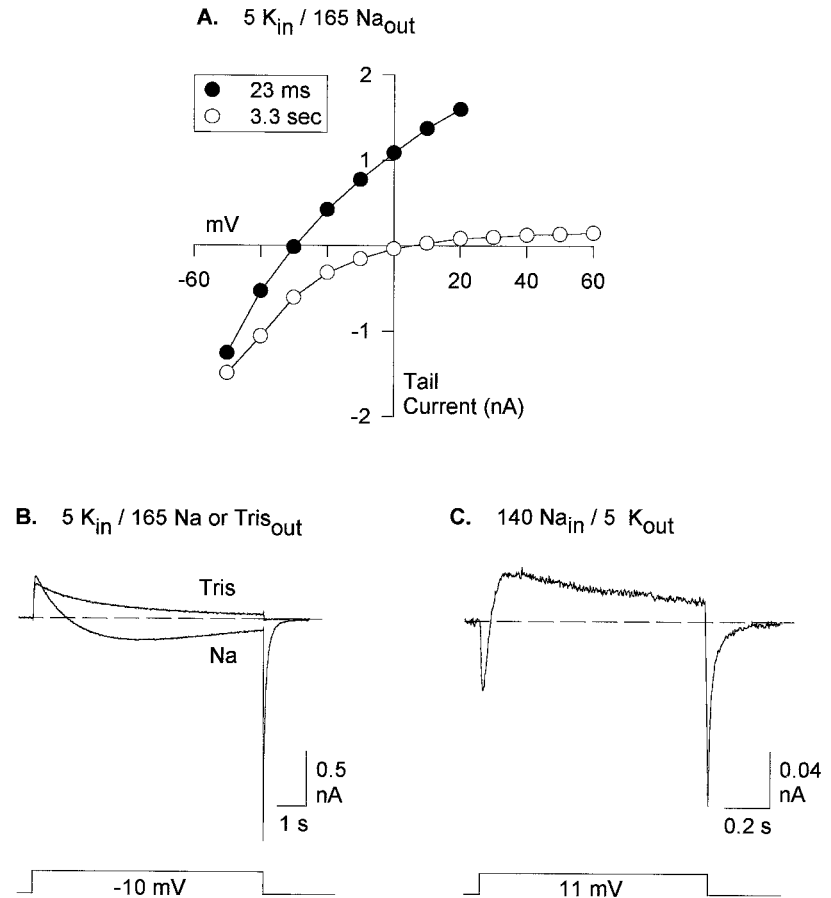
In the voltage-gated  $K^+$  channel, Kv2.1, ionic selectivity is determined at least partially by a competition between  $K^+$  and  $Na^+$  for occupancy of and passage through the pore (Korn and Ikeda, 1995). At high  $[K^+]$ ,  $Na^+$  currents are blocked. At lower  $[K^+]$ , currents through Kv2.1 are carried by a mixture of  $K^+$  and  $Na^+$ . With 30 mM internal  $K^+$  and 165 mM external  $Na^+$ , currents through Kv2.1 following channel activation for 88 ms reversed at  $-69$  mV (Fig. 1 A). This reversal potential represents a  $Na^+ : K^+$  permeability ratio of 0.012. Under these conditions, there was little inactivation. With more prolonged depolarization, channels inactivated and ionic selectivity changed, such that channels

became relatively more permeable to  $Na^+$  as  $K^+$  current decreased. Following a 4-second depolarization, channels inactivated by 63%, and the reversal potential shifted to  $-42$  mV (Fig. 1 B). Fig. 1 C plots current-voltage relationships at three different levels of inactivation from the cell in panels A and B. Fig. 1 D, which plots data from 13 cells, illustrates that the reversal potential shifted over 45 mV during the course of slow inactivation and that the reversal potential shift was positively correlated with percent inactivation. This shift represents approximately a 10-fold increase in  $Na^+$  permeability relative to  $K^+$ .

### Inward currents did not result from $K^+$ accumulation

The change in  $Na^+$  permeability associated with  $K^+$  current inactivation could also be observed with a different experimental protocol. Cells were depolarized for different durations, and the magnitude of inward current upon repolarization was monitored (Fig. 2 A). As outward  $K^+$  current inactivated, the magnitude of the inward current initially increased, as expected for an increase in relative  $Na^+$  permeability with  $K^+$  current inactivation. As the duration of depolarization was further increased,  $K^+$  current inactivation continued, and the inward tail current magnitude decreased. This biphasic change in inward current magnitude suggests that as inactivation proceeded, channels initially

FIGURE 3 Reversal of current through Kv2.1 over time. (A) Current magnitude as a function of repolarization potential, following 23 ms (solid circles) and 3.3 s (open circles) depolarization to +40 mV. Currents were recorded with 5 mM internal  $K^+$  and 0 external  $K^+$  (165 mM external  $Na^+$ ). (B) Currents recorded at  $-10$  mV with 5 mM internal  $K^+$  and 0 external  $K^+$ . One current was recorded in the presence of 165 mM external  $Na^+$  and the other in the absence of  $Na^+$  (Tris substitute). (C) Current recorded at  $+11$  mV with 0 internal  $K^+$  (140 mM internal  $Na^+$ ) and 5 mM external  $K^+$  (plus 165 mM Tris).



become more permeable to  $Na^+$  and then become less permeable to  $Na^+$ .

A possible artifactual explanation of the reversal potential shift (Fig. 1) and the enhanced inward tail current with prolonged depolarization (Fig. 2 A) was that  $K^+$  leaving the cell during depolarization accumulated outside the cell membrane and carried the inward current upon repolarization. We did two types of experiments to test for the possibility that external  $K^+$  accumulation contributed to the inward current.

First, we examined the inward current magnitude in the presence of increasing internal  $[K^+]$  (Fig. 2 A–C). If inward currents resulted from external accumulation of  $K^+$ , then extracellular accumulation of  $K^+$  should be greater, and the magnitude of inward current upon repolarization should be increased with higher internal  $[K^+]$ . This was not the case. With 5 mM internal  $K^+$  (Fig. 2 A), the largest inward tail current (trace 3) was  $1.57 \pm 0.20$  ( $n = 5$ ) times the magnitude of the outward  $K^+$  current. With an internal  $[K^+]$  of 30 mM, the inward tail current was just  $0.30 \pm 0.04$  ( $n = 4$ ) times the magnitude of the outward current (Fig. 2 B). With 100 mM internal  $K^+$ , no inward tail current was detectable (Fig. 2 C;  $n = 3$ ).

In the second type of experiment, we replaced external  $Na^+$  with  $NMG^+$ . As shown in Fig. 2 D, no inward tail current was observed despite prolonged activation of large

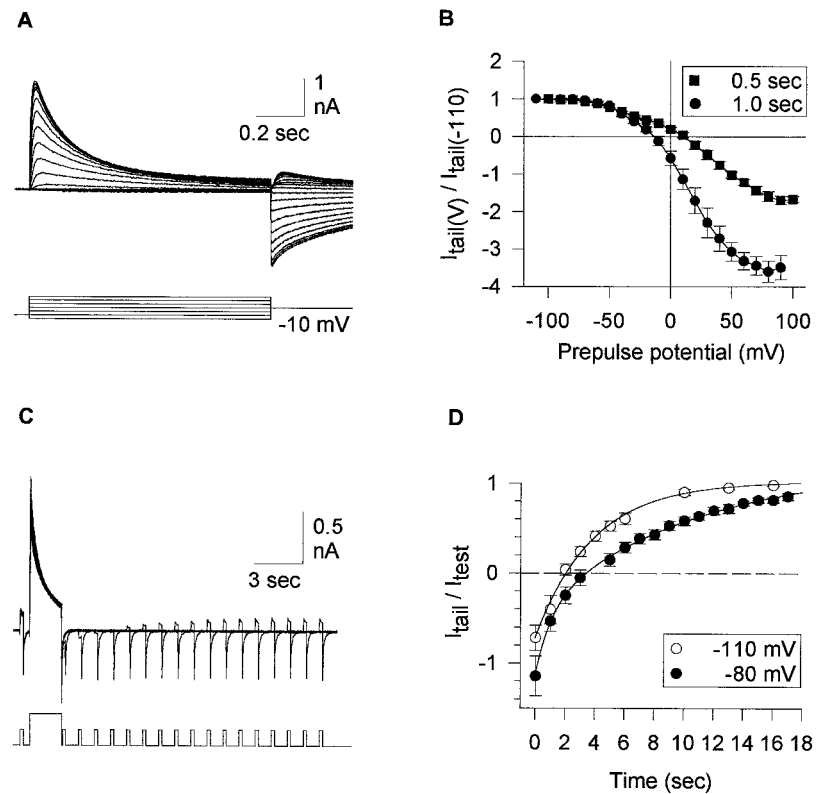
outward  $K^+$  currents. Similar experiments are illustrated in Fig. 3 B and Fig. 6 C. Taken together, these results demonstrate that the inward tail current was carried by  $Na^+$  and rule out the possibility that inward current was carried by  $K^+$  that had accumulated in the extracellular space during the depolarization-activated outward current.

### Inactivation as a multistep change in the permeation pathway

The reversal potential measurements in Fig. 1 indicated that with prolonged depolarization, the ability of  $Na^+$  to flow in the inward direction increased compared with the ability of  $K^+$  to flow in the outward direction. The experiments in Fig. 2 A and B suggested that as inactivation proceeded, the channel went through two permeation states. Initially, the ability of  $Na^+$  to conduct increased as the ability of  $K^+$  to conduct decreased. With more prolonged depolarization, the ability of  $Na^+$  to conduct then decreased. This was examined more directly in the experiments of Fig. 3.

With 5 mM internal  $K^+$  and 165 mM external  $Na^+$ , currents reversed at  $-30.5 \pm 2.5$  mV ( $n = 4$ ; Fig. 3 A, filled circles) following a brief depolarization in which no inactivation was observed. Following a 3.3-second depolarization that resulted in  $81.5 \pm 2.3\%$  inactivation, currents

**FIGURE 4** Change in selectivity and recovery from change in selectivity is voltage- and time-dependent. (A) Twin pulse protocol and currents that resulted (details described in text). (B) Peak tail currents measured following 0.5 and 1 s prepulse as a function of prepulse voltage. Currents were normalized to the peak outward tail current that followed the prepulse to  $-110$  mV ( $n = 3$  for each data set). (C) Protocol for studying recovery from inactivation and currents that resulted. An initial test depolarization to  $-10$  mV was presented to evoke a control outward  $K^+$  current. This was followed 400 ms later by a 2 s depolarization to  $+40$  mV to partially inactivate the channels. A test pulse to  $-10$  mV was then presented at 1 s intervals to monitor the recovery of the outward current. One postinactivation test pulse was delivered for each 2 s inactivating pulse; 17 superimposed currents are shown, recorded at 40 s intervals. (D) Time course of return from post-inactivation inward  $Na^+$  current to control outward  $K^+$  current, for two post-inactivation holding potentials ( $n = 7$  for each data set).



recorded under these conditions reversed at  $+4.5 \pm 1.7$  mV ( $n = 4$ ; Fig. 3 A, open circles). Because inactivation is a time-dependent phenomenon, depolarization to a single potential between the two reversal potentials would be predicted to produce an initial outward current carried by  $K^+$  that, over time, reverses to an inward current carried by  $Na^+$ . This was indeed the case. Depolarization to  $-10$  mV resulted in an initial outward current that reversed to an inward current in  $\sim 1$  s (Fig. 3 B). As the depolarizing stimulus continued, the inward current decayed, consistent with a transition to a state that allowed neither  $K^+$  nor  $Na^+$  to conduct. The inward current, but not the outward current, was eliminated upon replacement of external  $Na^+$  with the impermeant Tris (Fig. 3 B), which demonstrates that the inward current was carried by  $Na^+$ .

Similar results were obtained when the polarity of the current carrying ions was reversed (Fig. 3 C). With channels exposed externally to 5 mM  $K^+$  and internally to 140 mM  $Na^+$ , depolarization to  $+11$  mV resulted in an initial inward current, which reversed to an outward current as time progressed. As in Fig. 3 B,  $Na^+$  current decayed as depolarization continued, consistent with the transition to a non-conducting state. These data indicate that during inactivation, Kv2.1 channels convert from  $K^+$ -conducting to  $Na^+$ -conducting to nonconducting and therefore suggest that the conformational change that the channel goes through during inactivation is a multistep process.

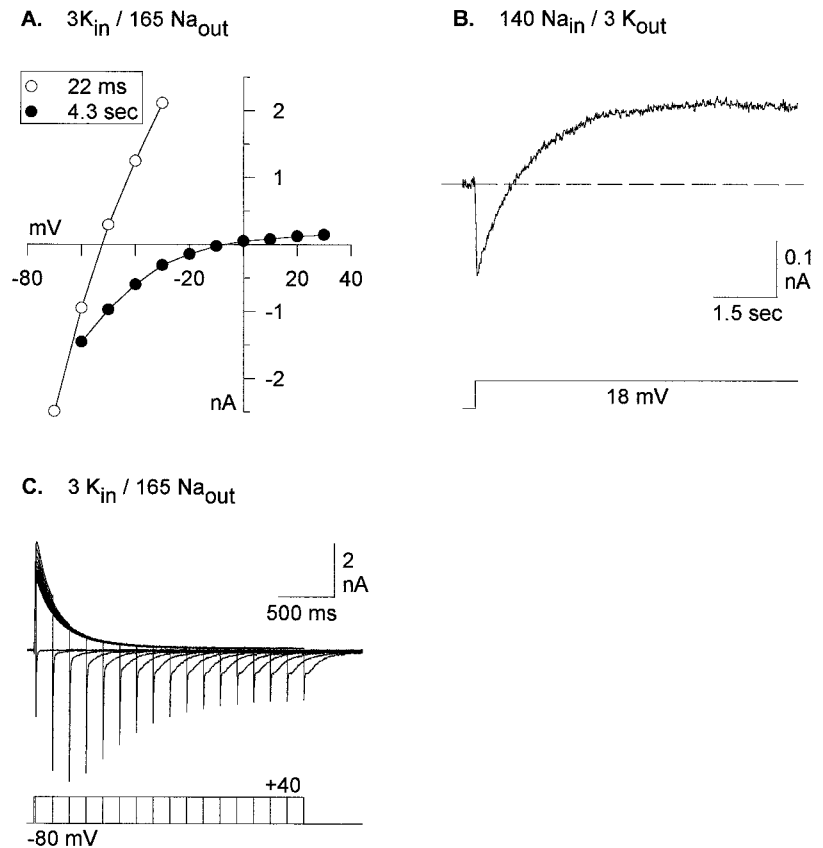
Reversal of current polarity occurred much more rapidly with  $K^+$  on the external side than the internal side of the membrane (compare Fig. 3 C with Fig. 3 B; the difference

in membrane potential in these two experiments would produce a negligible change in inactivation kinetics). With internal  $K^+$ , current reversed from outward to inward in  $912 \pm 111$  ms ( $n = 8$ ). With external  $K^+$ , current reversed from inward to outward in  $58 \pm 2$  ms ( $n = 3$ ). This suggests the presence of an asymmetry in the regulation of inactivation by  $K^+$ , possibly related to the location or number of  $K^+$  ions on either side of the selectivity filter (Doyle et al., 1998).

### Association of the selectivity change with the inactivation mechanism

Although the change in ionic selectivity in Kv2.1 over time appears to have been associated with the inactivation process, it remained a possibility that these two events represented independent responses to depolarization. We tested this by examining four properties classically associated with inactivation: voltage- and time-dependence of onset and voltage- and time-dependent recovery. Fig. 4 A illustrates the twin pulse protocols that were used to examine the voltage- and time-dependence of the onset of the selectivity change. Cells were held at potentials between  $-110$  and  $+90$  mV for 1 s, followed by a test pulse to  $-10$  mV. At  $-110$  mV, most or all channels should be removed from the inactivated state and initial current flow during the test pulse will represent current through the open state of the channel. Indeed, when cells were held for 1 s at  $-110$  mV, the test depolarization to  $-10$  mV evoked an outward  $K^+$  current.

**FIGURE 5** Change in selectivity during inactivation of a C-type inactivating, chimeric  $K^+$  channel. Recordings were made from a chimeric  $K^+$  channel that consisted of the S5-S6 loop from Kv1.3 inserted into the backbone of Kv2.1 (Kiss et al., 1998). (A) Tail currents were recorded as in Fig. 1 A, with 3 mM internal  $K^+$  and 165 mM external  $Na^+$ . Channels were activated by depolarization to +40 mV for 22 ms or 4.3 s. There was no apparent inactivation at 22 ms; the 4.3 s depolarization resulted in  $88.4 \pm 2.4\%$  ( $n = 6$ ) inactivation. (B) Current recorded as in Fig. 2 C, except with 140 mM internal  $Na^+$  and 3 mM external  $K^+$ . (C) Seventeen superimposed currents are illustrated, evoked at 20 s intervals under the ionic conditions of panel A. Depolarizations to +40 mV ranged in duration from 15 ms to 2.4 s at 150 ms intervals. Each depolarization was followed by repolarization to -80 mV. The peak inward  $Na^+$  tail current occurred on trace #3 in which the  $K^+$  current was inactivated by 74.8%.



As the prepulse was made more positive, the outward current evoked by the -10-mV test depolarization decreased in magnitude and eventually reversed to become an inward current. Fig. 4 B plots the current magnitude as a function of prepulse voltage for prepulses of 1 and 0.5 s duration. Current was normalized so that the peak outward current magnitude following a prepulse to -110 mV had a value of 1. As predicted for voltage-dependent inactivation, the change in selectivity was sensitive to both prepulse potential and time. Furthermore, as predicted for a slow inactivation mechanism, the magnitude of the inward  $Na^+$  current obtained following very positive prepulses was decreased with shorter duration prepulses.

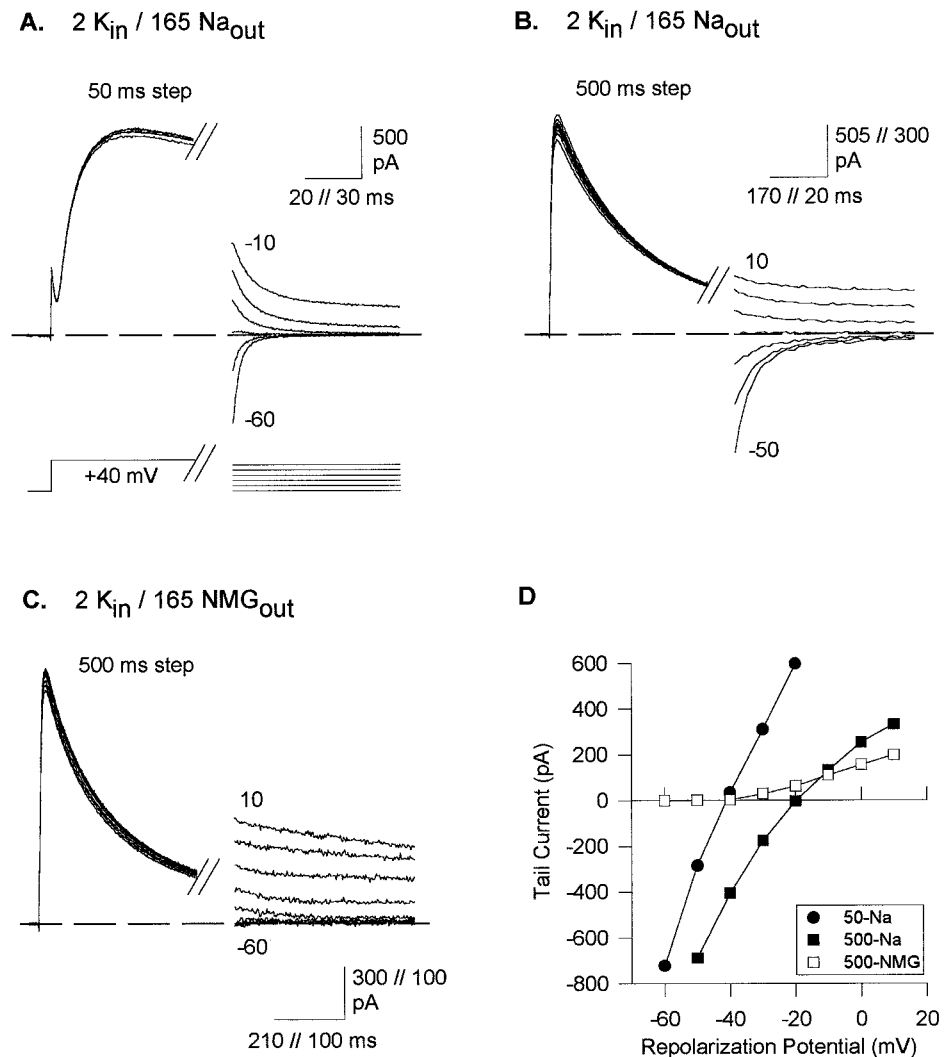
Fig. 4 C illustrates the protocol used to examine recovery from inactivation. A 200-ms test pulse to -10 mV was delivered to obtain the magnitude of outward  $K^+$  current before inactivation. A 2 s depolarization to +40 mV was then delivered 400 ms later to inactivate the channels (channels inactivated by  $83.8 \pm 1.3\%$ ,  $n = 7$ ), and then 200 ms test pulses to -10 mV were delivered at incremental intervals to monitor the recovery of the outward  $K^+$  current. Immediately following the 2 s inactivating stimulus, the current at -10 mV was inward. Over time, the magnitude of the inward current decreased and reversed to an outward current. Fig. 4 D illustrates the time-dependent recovery of  $K^+$  current for seven cells held at two different potentials. Similar to recovery from C-type inactivation in Kv1.3 (Levy and Deutsch, 1996), recovery from inward  $Na^+$  cur-

rent to within 10% of outward  $K^+$  current was both time and voltage-dependent; holding cells at more negative potentials during the recovery period increased the rate of recovery. The data in Fig. 4 indicate that the change in selectivity and the inactivation process are intimately linked, and suggest that indeed, the change in selectivity is caused by the inactivation process.

### Selectivity change in a C-type inactivating chimera

It has been proposed that slow inactivation in Kv2.1 has some properties that differ from classical C-type inactivation observed in *Shaker*, Kv1.3, and other  $K^+$  channels (De Biasi et al., 1993). Whether these differences represent variation of a single fundamental mechanism or represent a different inactivation mechanism has not yet been resolved. Because most of the mechanistic understanding of slow inactivation is derived from studies of channels that undergo classical C-type inactivation (Hoshi et al., 1991; Liu et al., 1996; Lopez-Barneo et al., 1993; Ogielska et al., 1995; Panyi et al., 1995; Yellen et al., 1994), we sought to determine directly whether the time-dependent change in selectivity observed in Kv2.1 also occurred in a channel undergoing C-type inactivation. These studies cannot be done with wild-type, C-type inactivating channels such as *Shaker*, or Kv1.3 because they are impermeable to  $Na^+$  in

**FIGURE 6** Change in current reversal potential in *Shaker*  $\Delta$  A463C during inactivation. Similar experiment to Fig. 1. (A) Tail currents recorded at repolarization potentials between  $-60$  and  $-10$  mV following 50 ms depolarizing steps to  $+40$  mV. (B) Tail currents recorded at repolarization potentials between  $-50$  and  $+10$  mV following 500 ms depolarizing steps to  $+40$  mV. (C) Identical experiment as panel B, except that external  $\text{Na}^+$  was replaced by  $\text{NMG}^+$ . (D) I-V curves, plotting tail current magnitude as a function of repolarization potential for the cells in A–C. Reversal potentials in the presence of external  $\text{Na}^+$ , averaged over 4 cells, were  $-41.5 \pm 1.3$  mV following the 50 ms depolarization and  $-20.3 \pm 3.0$  mV following the 500 ms depolarization.



the presence of even very low  $[\text{K}^+]$ . Consequently, we used a chimeric channel, composed of the S5–S6 loop from Kv1.3 inserted into a Kv2.1 backbone (Gross et al., 1994; Kiss et al., 1998). This channel allows  $\text{Na}^+$  to conduct better than Kv1.3, but like Kv1.3, appears to use a classical C-type inactivation mechanism (Kiss and Korn, 1998).

The current-voltage relationships in Fig. 5 A were obtained from chimeric channels recorded in the presence of 3 mM internal  $\text{K}^+$  and 165 mM external  $\text{Na}^+$ . Following brief (22 ms) depolarization, which produced little inactivation, currents reversed at  $-53.6 \pm 1.1$  mV ( $n = 9$ ; Fig. 5 A). Following a more prolonged (4.3 s) depolarization, which resulted in  $88.4 \pm 2.4\%$  ( $n = 6$ ) inactivation, current reversed at  $-11.8 \pm 1.3$  mV ( $n = 9$ ; Fig. 5 A). This represents a fivefold increase in permeability to  $\text{Na}^+$  relative to  $\text{K}^+$  following inactivation.

As observed in Kv2.1, this change in selectivity could also be observed as a time-dependent reversal of current polarity and could be observed with  $\text{K}^+$  on the extracellular side of the channel (Fig. 5 B). In the presence of 3 mM external  $\text{K}^+$  and 140 mM internal  $\text{Na}^+$ , current initially

flowed in the inward ( $\text{K}^+$ -carrying) direction and over time reversed to the outward ( $\text{Na}^+$ -carrying) direction. The results in Fig. 5 B appear to differ from those with Kv2.1 in that the outward  $\text{Na}^+$  current was sustained for a prolonged period of time. This observation is consistent with previous experiments, which demonstrated that  $\text{Na}^+$  continues to permeate this chimeric channel following inactivation (Kiss and Korn, 1998). However, the experiment in Fig. 5 C suggests that this chimeric channel also goes through two different permeation states during inactivation. Currents were recorded with 3 mM internal  $\text{K}^+$  and 165 mM external  $\text{Na}^+$  (as in Fig. 5 A), and depolarizing steps to  $+40$  mV were delivered for durations ranging from 15 ms to 2.4 s. Following a 15 ms depolarization, repolarization to  $-80$  mV revealed a small inward  $\text{Na}^+$  tail current. As inactivation progressed, peak inward tail currents became larger and then began to decrease, which reflects an initial increase followed by a decrease in inward  $\text{Na}^+$  conductance (inward currents were eliminated by removal of external  $\text{Na}^+$  and completely prevented by addition of 30 mM internal  $\text{K}^+$ , data not shown). Following prolonged depolarization,  $\text{Na}^+$

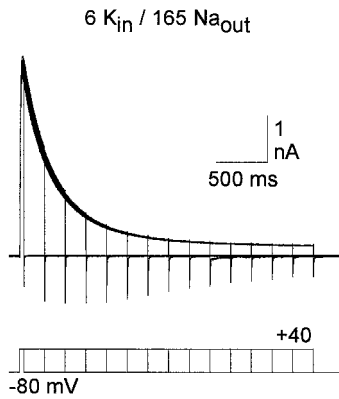


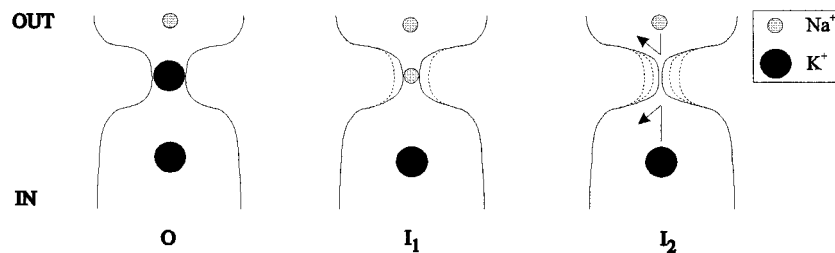
FIGURE 7 Biphasic change in  $\text{Na}^+$  current amplitude during inactivation in *Shaker*  $\Delta$  A463C. Protocol as in Fig. 2 A, except that the first depolarizing step was for a 40 ms duration, and the duration of subsequent steps increased in 200 ms increments. In three cells, the largest inward current (trace 3) was  $0.14 \pm 0.04$ , the size of the peak outward current.

continued to permeate the channel albeit with a reduced conductance. These data are consistent with the hypothesis that the chimeric channel, like Kv2.1, goes through two different inactivation states, which are distinguished by the relative ability of  $\text{Na}^+$  to permeate.

### Selectivity change in a *Shaker* mutant

Our data with the chimeric channel suggest that the selectivity change occurs in a C-type inactivating channel. However, this chimera is composed largely of Kv2.1 structural components (Kiss et al., 1998). Consequently, it could be argued that the selectivity change was still a unique function of the Kv2.1 structure. To test this, we examined the change in selectivity in a *Shaker* mutant, *Shaker*  $\Delta$  A463C. This channel is highly selective for  $\text{K}^+$ , allows  $\text{Na}^+$  to permeate in the absence of  $\text{K}^+$  better than wild-type *Shaker*, and displays competition between  $\text{K}^+$  and  $\text{Na}^+$  for passage through the pore (Ogielska and Aldrich, 1996). Fig. 6 illustrates tail currents in the presence of 2 mM internal  $\text{K}^+$ , following a 50-ms depolarization that produced little inactivation (Fig. 6 A) and a 500 ms depolarization (Fig. 6 B). The 500 ms depolarization resulted in  $74.0 \pm 5.6\%$  inactivation ( $n = 4$ ). In the absence of inactivation, currents reversed at  $-41.5 \pm 1.3$  mV ( $n = 4$ ; Fig. 6 A and D). Following the 500 ms depolarization, currents reversed at  $-20.3 \pm 3.0$  mV ( $n = 4$ ; Fig. 6 B and D). Substitution of NMG $^+$  for external  $\text{Na}^+$  abolished the inward currents (Fig. 6 C and D), which demonstrates that the inward current was carried by  $\text{Na}^+$  and was not due to extracellular accumulation of  $\text{K}^+$ .

#### A. Hypothesis I. The selectivity filter is the inactivation gate.



#### B. Hypothesis II. The inactivation gate is distinct from the selectivity filter.

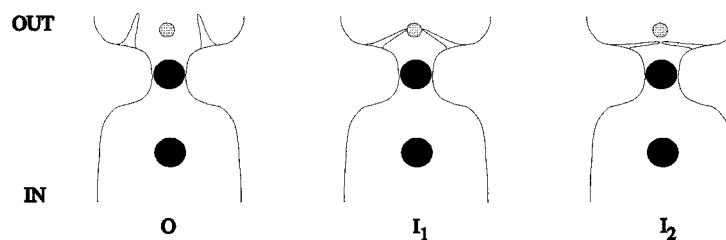


FIGURE 8 Schematic illustration of two hypotheses. The solid circles represent  $\text{K}^+$  ions, the hatched circles represent the smaller  $\text{Na}^+$  ions. For simplicity, the selectivity filter binding site is illustrated as occupied by a single ion. (A) Hypothesis I is that the selectivity filter itself is the inactivation gate. In the open state (state O),  $\text{K}^+$  is preferred over  $\text{Na}^+$ . During inactivation (state  $\text{I}_1$ ), the diameter of the narrow region of the pore decreases, inhibiting  $\text{K}^+$  flux but still allowing (and perhaps enhancing)  $\text{Na}^+$  flux. The presence of  $\text{K}^+$  in the inner vestibule does not prevent  $\text{Na}^+$  flux through the channel because of the relatively low affinity and nonselectivity of this site for cations (Bezanilla and Armstrong, 1972). As inactivation proceeds (state  $\text{I}_2$ ), the diameter of the narrow region decreases further and neither  $\text{K}^+$  nor  $\text{Na}^+$  can permeate the channel. (B) Hypothesis II is that the inactivation gate is external to and distinct from the selectivity filter. In this model, the structure that underlies the selectivity filter itself does not change during inactivation. During the initial phase of inactivation (state  $\text{I}_1$ ), a gate external to the selectivity filter starts to close, reaching an inner diameter that inhibits  $\text{K}^+$  flux but still allows  $\text{Na}^+$  to pass through the inactivation gate. In this state, however,  $\text{K}^+$  occupies a high affinity, highly selective cation site associated with the selectivity filter and prevents  $\text{Na}^+$  from conducting. State  $\text{I}_2$  would be indistinguishable from state  $\text{I}_1$  in our experiments.

As with Kv2.1 and the chimeric channel, *Shaker*  $\Delta$ A463C also displayed a biphasic change in  $\text{Na}^+$  permeation (Fig. 7). With 6 mM internal  $\text{K}^+$  and 165 mM external  $\text{Na}^+$ , the magnitude of the inward current increased as the outward  $\text{K}^+$  current inactivated by 70%. With prolonged depolarization and continued inactivation, the magnitude of the  $\text{Na}^+$  current then decreased. Inward  $\text{Na}^+$  currents were not observed with internal  $[\text{K}^+]$  greater than 10 mM (data not shown).

## DISCUSSION

When currents through  $\text{K}^+$  channels are carried by  $\text{K}^+$ , slow inactivation results in the virtually complete inhibition of current flow through the channel. The concept associated with this phenomenon, derived from the widely accepted description of changes in channel states as “gating” events, suggests the closing of a gate in the pore which stops the flow of current. Recently, conformational changes were demonstrated to occur in the outer mouth of the pore during inactivation (Yellen et al., 1994; Liu et al., 1996). The observations that all four subunits contribute to the inactivation mechanism (Ogielska et al., 1995; Panyi et al., 1995), that the rate of inactivation is decreased when the outer mouth of the channel is occupied by tetraethylammonium,  $\text{K}^+$ , or  $\text{H}^+$  (Busch et al., 1991; Choi et al., 1991; Lopez-Barneo et al., 1993; Baukowitz and Yellen, 1996), and that amino acids in the outer mouth of the pore become closer in proximity (Liu et al., 1996) suggested that the conformational change resulted in a constriction within the pore. Cysteine mutagenesis studies suggested that amino acids just external to the selectivity filter were involved in the molecular motion that contributed to the putative constriction (Yellen et al., 1994; Liu et al., 1996). The observation that ionic selectivity in the *Shaker*  $\text{K}^+$  channel changes during the slow inactivation process suggests that the molecular motion that underlies inactivation at least radiates to the selectivity filter (Starkus et al., 1997).

### Change in selectivity during slow (C-type) inactivation

Our results demonstrate that during slow inactivation, voltage-gated  $\text{K}^+$  channels undergo a multistep change in selectivity. Initially, the ability of  $\text{K}^+$  to conduct decreases and the permeability of  $\text{Na}^+$  relative to  $\text{K}^+$  increases. We cannot determine from our data whether the intrinsic ability of  $\text{Na}^+$  to conduct is enhanced during inactivation or whether the appearance of  $\text{Na}^+$  current reflects a decrease in the ability of  $\text{K}^+$  to block  $\text{Na}^+$  conductance as  $\text{K}^+$  permeability decreases. As inactivation continues, the ability of  $\text{Na}^+$  to conduct then decreases. Our data can be explained by either of two fundamentally different types of permeation state changes. First, during inactivation, the channel may change from one with a high selectivity for  $\text{K}^+$  (the open state), to one with a high selectivity for  $\text{Na}^+$  (inacti-

vation state one), to one that doesn't conduct (inactivation state two). Our data indicate that at all times during inactivation, the  $\text{Na}^+/\text{K}^+$  permeability ratio favors  $\text{K}^+$ . However, because the open,  $\text{K}^+$ -selective state has a very high conductance relative to any  $\text{Na}^+$  conducting state, simultaneous conduction through a small percentage (2–8%) of  $\text{K}^+$ -selective channels (channels in the open state) and a high percentage of  $\text{Na}^+$ -selective channels (inactivation state one) would result in a permeability ratio favoring  $\text{K}^+$ . Alternatively, during inactivation, the channel may proceed from the  $\text{K}^+$ -selective open state to a nonconducting state through one or more intermediate states that have intermediate permeability ratios for  $\text{K}^+$  and  $\text{Na}^+$ . Resolution of this issue will be aided by single channel measurements that cannot be made with currently available channels (single channel  $\text{Na}^+$ -conductance is too small).

In the discussion below, we present arguments for the hypothesis that the selectivity filter itself is an integral component of the inactivation gate. For simplicity, we have adopted the state transition model that includes just three discrete states, a  $\text{K}^+$ -conducting state, a  $\text{Na}^+$ -conducting state, and a nonconducting state, with the understanding that our interpretations would apply equally to a model that included intermediate states with intermediate  $\text{Na}^+/\text{K}^+$  permeability ratios.

### Evidence that the selectivity filter is the inactivation gate

Occupation of the pore by  $\text{K}^+$  slows inactivation (Lopez-Barneo et al., 1993; Baukowitz and Yellen, 1996) apparently by binding to a high affinity site associated with the ionic selectivity mechanism (Kiss and Korn, 1998). Structural data suggest that this high affinity binding occurs in the narrow region of pore that constitutes the selectivity filter (Doyle et al., 1998). These observations suggested that the slow inactivation process involved the selectivity filter.

Our data presented here support the hypothesis that the selectivity filter itself is part of, and possible solely, the inactivation gate (Fig. 8 A) and argue against the hypothesis that the inactivation gate is independent of the selectivity filter. As inactivation proceeds, the ability to conduct  $\text{K}^+$  decreases and the ability to conduct  $\text{Na}^+$  increases. In appropriate mixtures of  $\text{K}^+$  and  $\text{Na}^+$ , the channel changes from a state that carries predominantly  $\text{K}^+$  to a state that carries predominantly  $\text{Na}^+$  (Fig. 3 B and C). Subsequently, the channel proceeds from a  $\text{Na}^+$ -conducting state to a nonconducting state (Fig. 3 B and C). These data are consistent with a model whereby the conformational change during inactivation proceeds by a multistep process, during which the selectivity filter properties change at least twice. In the simplest (but not the only) possible model (Fig. 8 A), the open state (state O) is highly selective for  $\text{K}^+$  over  $\text{Na}^+$ . During inactivation, the channel converts to a state (state  $I_1$ ) that significantly inhibits or prevents  $\text{K}^+$  flow through the selectivity filter but which conducts  $\text{Na}^+$  relatively well. As

inactivation continues (state  $I_2$ ), the ability of  $\text{Na}^+$  to conduct is then diminished. It should be noted that, in accord with previous hypotheses, the model is drawn to suggest that the conformational change results in a constriction of the selectivity filter. The most important point, however, is that in order for inactivation to occur, this hypothesis requires that the ability of  $\text{K}^+$  to occupy the selectivity filter, from either the internal vestibule or external vestibule, is markedly reduced.

### Evidence that the inactivation gate is not independent from the selectivity filter

Previous data were also, however, consistent with an alternative hypothesis, that inactivation inhibits current flow at a pore location distinct from (and external to) the selectivity filter. In this case, the change in ionic selectivity could result from at least two possible mechanisms. First, a change in selectivity filter properties could be secondary to the molecular motion that underlies inactivation at the more external location. Thus, the molecular motion that closes the inactivation gate might radiate to the selectivity filter, and the change in selectivity would then be a by-product of inactivation. Alternatively, conformational changes that occur remote from the "selectivity filter" could, indeed, produce a change in ionic selectivity. For example, if both  $\text{Na}^+$  and  $\text{K}^+$  are capable of passing through the selectivity filter, then the relative ability of  $\text{Na}^+$  and  $\text{K}^+$  to reach the selectivity filter will influence the relative permeability. Thus, a conformational change that occurs in the permeation pathway leading to the selectivity filter could initially decrease access of  $\text{K}^+$  to the selectivity filter while enhancing or not changing the ability of  $\text{Na}^+$  to reach the selectivity filter. If this occurred, the permeability of  $\text{Na}^+$  relative to  $\text{K}^+$  would increase. Although it has not been ruled out, there is no experimental support for the hypothesis that a conformational change occurs internal to the selectivity filter during slow inactivation. In theory, however, an inactivation-induced conformational change in the external vestibule, for which there is substantial evidence, could produce such a change in selectivity. For example, channels respond functionally to millimolar concentrations of extracellular  $\text{K}^+$ , consistent with the presence of a low affinity  $\text{K}^+$  "binding site" external to the selectivity filter (Baukowitz and Yellen, 1996; Levy and Deutsch, 1996; Lopez-Barneo et al., 1993; Kiss and Korn, 1998). Whether this low affinity binding site is associated with the doubly bound GYG sequence, as intimated by Doyle et al. (1998), or reflects a poorly understood  $\text{K}^+$  concentrating mechanism external to the GYG sequence, is not yet known. Nonetheless, a substantial change in the functional properties of this external binding site, such that access of external  $\text{Na}^+$  to the selectivity filter increased dramatically during inactivation, could increase the relative permeability of  $\text{Na}^+$  and thus produce the observed increase in selectivity.

The data in Figs. 3 *B* and *C* and 5 *B* argue against the hypothesis that the inactivation gate is distinct from the

selectivity filter. As inactivation proceeds in relatively low  $[\text{K}^+]$ , channels convert from predominantly  $\text{K}^+$  conducting (currents flowing with the  $[\text{K}^+]$  gradient) to predominantly  $\text{Na}^+$  conducting (currents flowing against the  $[\text{K}^+]$  gradient). In these two different states, the selectivity filter is primarily occupied by  $\text{K}^+$  and  $\text{Na}^+$ , respectively. If the inactivation gate were located on one side of the selectivity filter and distinct from the selectivity filter, one would expect to observe the inactivation-induced change in selectivity with  $\text{K}^+$  on one side of the pore but not the other. This is depicted in Fig. 8 *B*, which illustrates a pore with an inactivation gate external to the selectivity filter. A conformational change at this externally located gate could produce a relative increase in access of  $\text{Na}^+$  to the selectivity filter (Fig. 8 *B*,  $I_1$ ). For example, such a conformational change could preferentially concentrate  $\text{Na}^+$  at the approach to the selectivity filter, and possibly also reduce the effective  $[\text{K}^+]$  in this region. With  $\text{K}^+$  on the side of the channel opposite the gate (the internal side, in this case),  $\text{K}^+$  would continue to gain unimpeded access to the selectivity filter (Fig. 8 *B*,  $I_1$ ). The affinity of the selectivity filter for  $\text{K}^+$  is much higher than for  $\text{Na}^+$  (in the chimera,  $100 \mu\text{M}$   $\text{K}^+$  is sufficient to block current carried by  $165 \text{ mM}$   $\text{Na}^+$ ; Kiss and Korn, 1998) and according to this hypothesis, would not change with inactivation. Consequently, occupancy of the selectivity filter by  $\text{K}^+$  would continue to prevent  $\text{Na}^+$  from flowing through the channel in the inactivated state. Because the inactivation process inhibits  $\text{K}^+$  flux and enhances relative  $\text{Na}^+$  flux regardless of whether  $\text{K}^+$  is internal or external to the selectivity filter, either the selectivity filter itself must be responsible for the inhibition of  $\text{K}^+$  flux or there must be two inactivation gates, one on either side of the selectivity filter.

### Mechanism of selectivity for $\text{K}^+$ over $\text{Na}^+$

Our data also provide experimental evidence for the mechanism of ionic selectivity in  $\text{K}^+$  channels. The "close fit hypothesis", proposed to explain ionic selectivity in  $\text{K}^+$  channels (Bezanilla and Armstrong, 1972), postulates that the ability of  $\text{K}^+$  but not  $\text{Na}^+$  to traverse the selectivity filter occurred because  $\text{K}^+$  fits snugly within the narrow region of the pore and could bind strongly with a cation binding site associated with the narrow region. In contrast  $\text{Na}^+$  was too small to fit snugly into the narrow region and could not obtain enough energy to dehydrate and conduct. Doyle et al. (1998) interpreted their structural model of the *Streptomyces lividans*  $\text{K}^+$  channel as evidence for a rigid selectivity filter and again proposed that selectivity against  $\text{Na}^+$  resulted largely from the inability of  $\text{Na}^+$  to fit snugly enough within the selectivity filter to dehydrate. Combined with evidence that the pore undergoes a constriction during inactivation, the observation that channel selectivity shifts from nearly exclusive preference for the larger  $\text{K}^+$  to a significant facility for conducting the smaller  $\text{Na}^+$  (or  $\text{Li}^+$ , data not shown) to a nonconducting channel provides func-

tional experimental support for this hypothesis. However, these results also suggest that the selectivity filter structure is not entirely rigid.

## Summary

Slow inactivation in Kv2.1 is clearly different from “classical” C-type inactivation. However, our data suggest that one underlying mechanism in common to slow inactivation in both Kv2.1 and *Shaker*-related channels is that the functional properties of the selectivity filter undergo a multi-step change, such that the channel initially becomes less permeable to K<sup>+</sup> and relatively more permeable to Na<sup>+</sup> and then as the inactivation process continues, becomes less permeable to Na<sup>+</sup>.

We thank Dr. Richard Horn for critically reading the manuscript and Drs. Carol Deutsch and Richard Horn for valuable discussions. We thank Dr. Rod MacKinnon for giving us cDNA for the chimeric channel and Dr. Gary Yellen for giving us cDNA for *Shaker* Δ A463C.

This work was supported in part by the National Science Foundation and the UCONN Research Foundation.

## REFERENCES

- Aldrich, R. W. 1981. Inactivation of voltage-gated delayed potassium current in molluscan neurons. *Biophys. J.* 36:519–532.
- Aldrich, R. W., P. A. Getting, and S. H. Thompson. 1979. Mechanism of frequency-dependent broadening of molluscan neurone soma spikes. *J. Physiol.* 291:531–544.
- Baukowitz, T., and G. Yellen. 1996. Use-dependent blockers and the exit rate of the last ion from the multi-ion pore of a K<sup>+</sup> channel. *Science* 271:653–656.
- Bezanilla, F., and C. M. Armstrong. 1972. Negative conductance caused by entry of sodium and cesium ions into the potassium channels of squid axons. *J. Gen. Physiol.* 60:588–608.
- Busch, A. E., R. S. Hurst, R. A. North, J. P. Adelman, and M. P. Kavanaugh. 1991. Current inactivation involves a histidine residue in the pore of the rat lymphocyte potassium channel RGK5. *Biochem. Biophys. Res. Commun.* 179:1384–1390.
- Choi, K. L., R. W. Aldrich, and G. Yellen. 1991. Tetraethylammonium blockade distinguishes two inactivation mechanisms in voltage-gated K<sup>+</sup> channels. *Proc. Natl. Acad. Sci. USA* 88:5092–5095.
- De Biasi, M., H. A. Hartmann, J. A. Drewe, M. Tagliatalata, A. M. Brown, and G. E. Kirsch. 1993. Inactivation determined by a single site in K<sup>+</sup> pores. *Pflugers Archiv.* 422:354–363.
- Doyle, D. A., J. M. Cabral, R. A. Pfuetzner, A. Kuo, J. M. Gulbis, S. L. Cohen, B. T. Chait, and R. MacKinnon. 1998. The structure of the potassium channel: molecular basis of K<sup>+</sup> conduction, and selectivity. *Science.* 280:69–77.
- Grissmer, S., and M. Cahalan. 1989. TEA prevents inactivation while blocking open K<sup>+</sup> channels in human T lymphocytes. *Biophys. J.* 55:203–206.
- Gross, A., T. Abramson, and R. MacKinnon. 1994. Transfer of the scorpion toxin receptor to an insensitive potassium channel. *Neuron.* 13: 961–966.
- Heginbotham, L., and R. MacKinnon. 1992. The aromatic binding site for tetraethylammonium ion on potassium channels. *Neuron.* 8:483–491.
- Hoshi, T., W. N. Zagotta, and R. W. Aldrich. 1990. Biophysical and molecular mechanisms of *Shaker* potassium channel inactivation. *Science.* 250:533–538.
- Hoshi, T., W. N. Zagotta, and R. W. Aldrich. 1991. Two types of inactivation in *Shaker* K<sup>+</sup> channels: effects of alterations in the carboxy-terminal region. *Neuron.* 7:547–556.
- Hsu, H. E., E. Huang, X-C. Yang, A. Karschin, C. Labarca, A. Figl, B. Ho, N. Davidson, and H. A. Lester. 1993. Slow and incomplete inactivations of voltage-gated channels dominate encoding in synthetic neurons. *Biophys. J.* 65:1196–1206.
- Jurman, M. E., L. M. Boland, Y. Liu, and G. Yellen. 1994. Visual identification of individual transfected cells for electrophysiology using antibody-coated beads. *Biotechniques.* 17:876–881.
- Kiss, L., D. Immke, J. LoTurco, and S. J. Korn. 1998. The interaction of Na<sup>+</sup> and K<sup>+</sup> in voltage-gated potassium channels. Evidence for cation binding sites of different affinity. *J. Gen. Physiol.* 111:195–206.
- Kiss, L., and S. J. Korn. 1998. Modulation of C-type inactivation by K<sup>+</sup> at the potassium channel selectivity filter. *Biophys. J.* 74:1840–1849.
- Korn, S. J., and S. R. Ikeda. 1995. Permeation selectivity by competition in a delayed rectifier potassium channel. *Science.* 269:410–412.
- Levy, D. I., and C. Deutsch. 1996. Recovery from C-type inactivation is modulated by extracellular potassium. *Biophys. J.* 70:798–805.
- Liu, Y., M. E. Jurman, and G. Yellen. 1996. Dynamic rearrangement of the outer mouth of a K<sup>+</sup> channel during gating. *Neuron.* 16:859–867.
- Lopez-Barneo, J., T. Hoshi, S. H. Heinemann, and R. W. Aldrich. 1993. Effects of external cations and mutations in the pore region on C-type inactivation in *Shaker* potassium channels. *Receptors and Channels.* 1:61–71.
- MacKinnon, R., and G. Yellen. 1990. Mutations affecting TEA blockade and ion permeation in voltage-activated K<sup>+</sup> channels. *Science.* 250: 276–279.
- Marom, S., and I. B. Levitan. 1994. State-dependent inactivation of the Kv3 potassium channel. *Biophys. J.* 67:579–589.
- Ogielska, E. M., and R. W. Aldrich. 1996. Mutations in the S6 segment of *Shaker* channels allow sodium permeation in the absence of potassium. *Biophys. J.* 70:A191.
- Ogielska, E. M., W. N. Zagotta, T. Hoshi, S. H. Heinemann, J. Haab, and R. W. Aldrich. 1995. Cooperative subunit interactions in C-type inactivation in K channels. *Biophys. J.* 69:2449–2457.
- Panyi, G., Z. Sheng, L. Tu, and C. Deutsch. 1995. C-type inactivation of a voltage-gated K<sup>+</sup> channel occurs by a cooperative mechanism. *Biophys. J.* 69:896–903.
- Starkus, J. G., L. Kuschel, M. Rayner, and S. H. Heinemann. 1997. Ion conduction through C-type inactivated *Shaker* channels. *J. Gen. Physiol.* 110:539–550.
- Stuhmer, W., J. P. Ruppersberg, K. H. Schroter, B. Sakmann, K. Stocker, P. Giese, A. Perschke, A. Baumann, and O. Pongs. 1989. Molecular basis of functional diversity of voltage-gated potassium channels in mammalian brain. *EMBO J.* 8:3235–3244.
- Yellen, G., D. Sodickson, T-Y. Chen, and M. E. Jurman. 1994. An engineered cysteine in the external mouth of a K<sup>+</sup> channel allows inactivation to be modulated by metal binding. *Biophys. J.* 66: 1068–1075.
- Zagotta, W. N., T. Hoshi, and R. W. Aldrich. 1990. Restoration of inactivation in mutants of *Shaker* K<sup>+</sup> channels by a peptide derived from ShB. *Science.* 250:568–571.